
THE $H_xLi_{1-x}TaWO_6 \cdot nH_2O$ TRIRUTILE STRUCTURE CHARACTERIZATION THROUGH RAMAN AND IR SPECTRA COMPARISON: THE NON-CENTER SYMMETRIC CASE

A PREPRINT

D. Valim¹, AG Souza Filho,² J M Filho,²

¹Faculdade de Ciências Exatas e Tecnologia,
Universidade do Estado de Mato Grosso,

²Departamento de Física, Universidade Federal do Ceará,

*daniel.valim@unemat.br

OL Alves,³ MAC de Santis,³ E N Silva⁴

³Departamento de Química-UNICAMP/Campinas, Brazil

⁴Departamento de Física, Universidade Federal do Maranhão, São Luís, Brazil

November 28, 2021

ABSTRACT

We have performed the $LiTaWO_6$ vibrational studies for both Raman and infrared active modes. Although we do not have crystalline samples, the study was conducted qualitatively, firstly comparing the sample with similar compounds in the literature, and secondly comparing both Raman and infrared spectra of the $LiTaWO_6$ compound. Although the procedure is limited, we can assign 8 of the 10 Raman-IR active modes expected by Group Theory.

Keywords Trirutile · Non-center Symmetric · Raman active modes · IR active modes

1 Introduction

We can understand the trirutile structure like a normal rutile superlattice[1]. The standart composition is $A_{1/3}B_{2/3}O_2$ or AB_2O_6 where cations A^{n+} and B^{m+} where in under the condition of $n+2m = 12$ equation. The possible combinations for n and m are $n = 6, m = 3$ and $n = 2, m = 5$. For this cases, the difference of three charge units($m - n = 3$) is enough to ionic ordering three times the normal rutile c axis. The trirutile Space Group is the same as simple rutile $P4_2/mnm(D_{4h}^{14})$, $Z = 2$. In this Group A and B cations occupy $2a(000)$ and $4e(00z)$ Wyckoff positions, respectively, while there two non-equivalent Wyckoff positions for $4f(xx0)$ and $8j(xxz)$ of oxygens. A distorted trirutile structure ($P2_1/n$), whose is a $P4_2/mnm$ subgroup, was found for SnO_2 , $CrTa_2O_6$ [2, 3, 4, 5] and $CuSb_2O_6$ compounds[6].

The $LiMWO_6$ ($M = Ta, W$) compound belongs to a family material with chemical formula like $AB'B''O_6$, where A, B' and B'' are monovalent, three and hexavalent, respectively. In 1970, Blasse and Paw[7] proposed the these materials belong to tetragonal center-symmetric structure to $LiTaWO_6$ $P4_2/m(D_{2d}^3)$ (with $a = b = 4.6776, c = 9.0337$ Å). Fourquet et.al.[8] proposes the non-center symmetric Space Group $P\bar{4}2_1m(D_{2d}^3)$ (with $a = b = 4.6776, c = 9.2710$ Å) for $LiTaWO_6$ compound. More recently, in 2002, Catti[9] proposed a new structure to this compound, obtaining an orthorhombic center-symmetric $Cmmm(D_{2h}^{19})$ (with $a = b = 6.6088$ and $c = 9.2999$ Å) with volume approximately two times the ones before proposed. In this work the $HTaWO_6 \cdot H_2O$ trirutile was refined to $P4_2/mnm(D_{4h}^{14})$ Space Group.

In all cases, the $\text{LiTaWO}_6 \cdot \text{H}_2\text{O}$ trirutile is constituted by LiO_6 , TaO_6 and WO_6 octahedras connected like showed in Figure 2. Note that due to the octahedra ordering, Li, Ta and W cations are disposed parallel to c axis.

As a matter of fact, the $P4_2/mnm$, $P\bar{4}2_1m$ and $Cmmm$ Space Groups obey the well defined Group-subgroup mathematical relationships, when a reduction of symmetry of $P4_2/mnm$ or $Cmmm$ must be splitting of Wyckoff positions as showed in Table 2.

The introduction of two similar size cations in B site positions can result in ordering of structure as occur to LiTaWO_6 trirutile. It means that taking in account the Space Group correlation between $P4_2/mnm$ and $P\bar{4}2_1m$ there are two non-equivalent positions to B cations and three non-equivalent positions to oxigen anions.

It is known that HTaWO_6 crystallizes in two different structures, a defect pyrochlore and trirutile. The defect pyrochlore one can be obtained via ionic change of its alkaline compound counterpart. In this case it is the KTaWO_6 compound. Instead, the HTaWO_6 trirutile is formed by anion change reaction from LiTaWO_6 of same structure.

Buvanesh et. al. [10] has been studied non-linear optic responses of $\text{LiM}^V\text{M}^{VI}\text{O}_6$ ($\text{M}^V=\text{Nb}$, Ta ; $\text{M}^{VI}=\text{Mo}$, W) polycrystalline samples with 25-45 μm grain sizes. It was demonstrated that materials exhibit SHG (Second Harmonic Generation) of 1064 nm wavelength radiation with efficiency of 16-28 times bigger than α -quartz. We know that, SHG is allowed only to non-center-symmetric samples what is consistent with Space Group described above ($P\bar{4}2_1m$).

2 Experimental Characterization

2.1 Synthesis

The reactants used to prepare LiTaWO_6 precursor samples are shown in Table 1. The synthesis of LiTaWO_6 Trirutile precursor was based in the procedure described by Catti[11] using stoichiometric reaction with following reactants:

Reactant	Formula	Manufacturer	Purity(%)
Tantalum Dioxide	Ta_2O_5	Alfa	99
Tungsten Dioxide	WO_3	Aldrich	99
Lithium Carbonate	Li_2CO_3	Vetec	99
Nitric Acid	HNO_3	Merck	65*

*Aqueous solution concentration.

Table 1: Reactants used to trirutile samples synthesis.

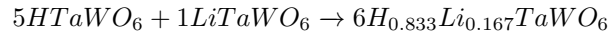
, with following reaction describe bellow:



The reactants were crushed and mixed in an agate mortar for 10 minutes, and after the mixing was transferred for a Platine crucible to heating at 850 °C in an oven. The system remains under heating by 24 hours, with an interruption after 12 hours for crushing and homogenization of the mixing.

The LiTaWO_6 Trirutile precursor was submitted at ionic exchange reactions in HNO_3 4mol.L⁻¹ solution for 48 h, at 80 °C. The supernatant solution was exchanged in an analogous way describe in reference[12] to Pyrochlore synthesis. The used acids and experimental parameters are based on procedures described in the literature[13, 11]. We have performed Li^+/H^+ ionic exchange reactions in LiTaWO_6 precursor to yield the HTaWO_6 trirutile.

Finally, the protonated compounds were again subjected to ion exchange reactions, this time the proton was replaced by Li^+ ions. The reactions were performed using the procedures of LQES laboratory for similar compounds[14, 15]. For this time, the reactions were performed by only one Li:H molar ration of 1:5 to form $\text{H}_x\text{Li}_{1-x}\text{TaWO}_6$. We know the ion exchange reaction, to 1:5 for example, occurs as follows



Where we can adjust the x, which is the concentration ratio of lithium to 0.167, wich result $\text{H}_{0.833}\text{Li}_{0.167}\text{TaWO}_6 \cdot n\text{H}_2\text{O}$ trirutile compound. This procedure is analogous to that described in the references[16, 17].

2.2 X-ray diffraction

The X-ray diffractogram were obtained in a Shimadzu diffractometer, operating in scan mode with $\text{CuK}\alpha$ radiation, generated at 40 KV and 30 mA current. The scanning speed used was 2/min in 2θ , with accumulation for reading every 0.6 seconds. The slits were used: divergent 1.0 mm and collection 0.3 mm. The calibration of the scanning angle was done with polycrystalline silicon and the samples were analyzed in powder form.

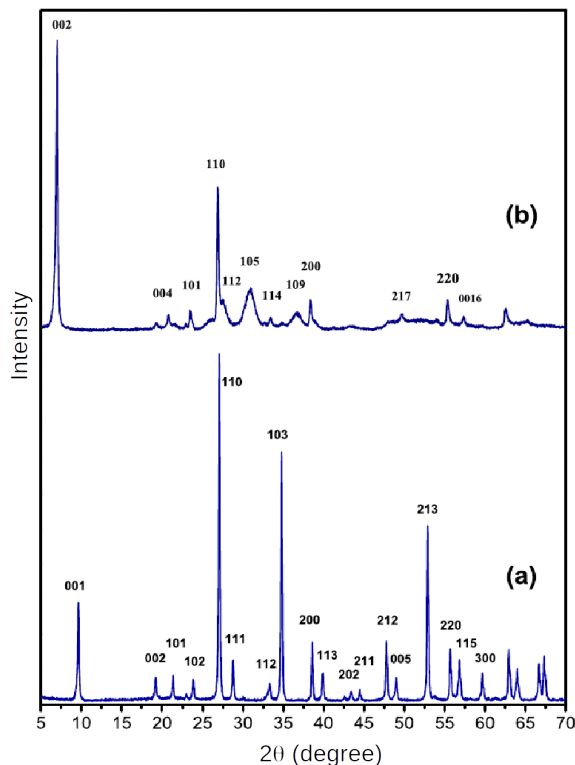


Figure 1: X-ray diffractograms of compounds in the trirutile structure $P\bar{4}2_1m (D_{2d}^3)$: (a) LiTaWO_6 (b) $\text{HTaWO}_6 \cdot n\text{H}_2\text{O}$ [12].

2.3 FTIR spectroscopy

The Fourier Transform Infrared (FTIR) spectra were obtained by Bomen ABB-FTLA 2000 in the $250\text{-}4000\text{ cm}^{-1}$ interval with 4 cm^{-1} resolution and 16 accumulations. The samples were studied in KBr pellets from Fluorolube dispersion, for spectra in the $1300\text{-}4000\text{ cm}^{-1}$, and in Nujol, for $250\text{-}1300\text{ cm}^{-1}$, using cesium-iodide windows. The FTIR measurements were made in the LQES laboratory[12].

2.4 Raman spectroscopy

All spectra measurements had been performed at room temperature through following experimental apparatus: an Argon laser, a Jobin Yvon T64000 three-monochromator spectrometer equipped by a microscope with 180 mm of focal objective. The laser line was 488 nm with power of 300 mW on the trirutile samples.

3 Results and Discussions

3.1 X-ray diffraction

The ionic exchange does not change the structure of the compound, like is showed in the diffractograms of **Figure 1** wich structures correspond that showed in the Figure 2. The ionic exchange Li^+/H^+ in the trirutile structure, the

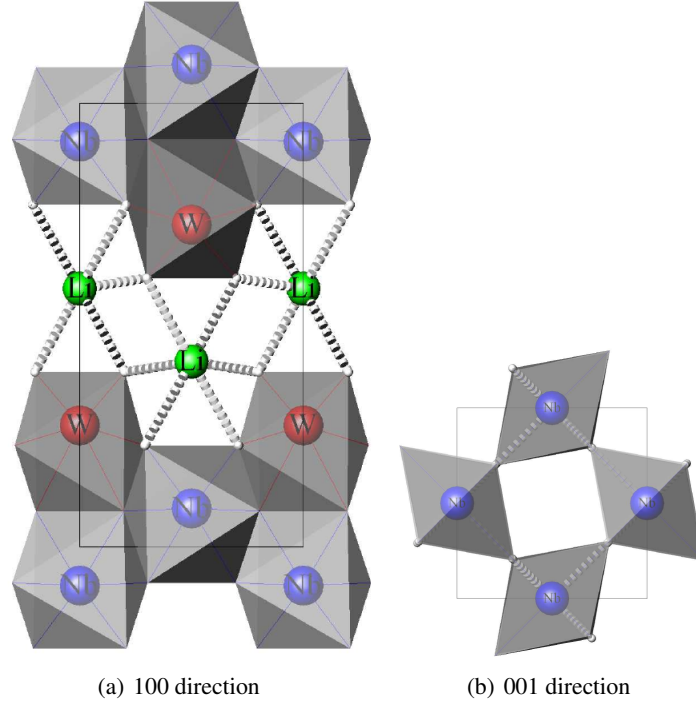


Figure 2: Unit cell projections of $P\bar{4}2_1m$ (D_{3d}^3) Space Group of LiNbWO_6 compound [8] at long (a) [100] and (b) [001] directions.

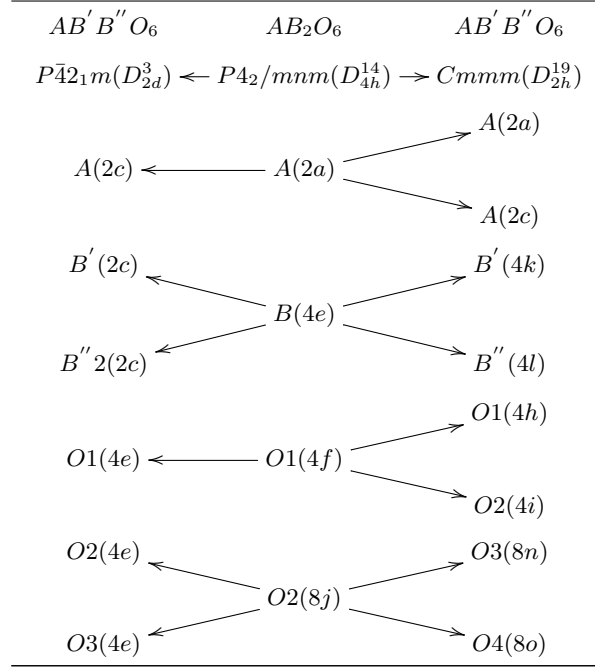
tetragonal crystalline system produce the expansion of the cell c parameter from 9.24 to 25.52 Å, as we can verify by Miller index $00l$. Instead of, we got a significant dislocation of 002 peak position, while the 110 peak position remains unaltered.

For a lot of authors, the c parameter expansion is the primary evidence of tetragonal cell remaining after ionic exchange reactions[18, 19, 20]. The formation of supercell can be attributed to interlayers translations of water molecules, perpendicular to the c axis, that were oriented to optimize hydrogen bonds connected to adjacent layers[19]. A thorough analysis of the characteristics of that reactions has shown that Li^+/H^+ exchange reactions process occur together with a tetragonal primitive (LiTaWO_6) to tetragonal body-center($\text{HTaWO}_6 \cdot \text{H}_2\text{O}$) transformation[18].

In the **Figure 1** are showed the X-ray diffractogram of both trirutile pristines $\text{HTaWO}_6 \cdot n\text{H}_2\text{O}$ and LiTaWO_6 of the reference [12]. The ionic change Li^+/H^+ in the trirutile structure produce the cell expansion in the parameter c , from 9.27 Å to 25.62 Å like verified by Miller index shift 001. In spite of remarkable shift of 002 peak, the position of 110 diffraction peak remains unchanged. For the majority of authors, it is the main evidence of tetragonal cell keeping after ionic change[18, 19, 20].

The formation of superlattice is assign at translation of interlamellar layers, perpendicular at c -axis, because introduction of water molecules into structure [18, 19]. The ionic change Li^+/H^+ in compound, also cause alteration of primitive tetragonal unit cell to body centered tetragonal, when $\text{HTaWO}_6 \cdot n\text{H}_2\text{O}$ is its hydrated form ($x = 3/2 > n > 1/2$)[18]. The structure maintenance after Li^+/H^+ ionic change, reveals high bi-dimensional mobility of precursor lithium, confirmed by studies of its diffusion coefficient [21].

Table 2: Outspread of Wyckoff positions from trirutile structures (D_{4h}^{14}) to similars (D_{2d}^3) and (D_{2h}^{19}).



4 Group Theory and vibrational spectroscopy

In the case of $ABBO_6$ compounds, the Table 3 shows 54 degrees of freedom through D_{2d} representation Factor Group of $P\bar{4}2_1m$ Space Group ($Z = 2$). From all modes ($9A_1 + 3A_2 + 3B_1 + 9B_2 + 15E$) the $9A_1 + 3B_1 + 8B_2 + 14E$ are Raman active modes, while the $8B_2 + 14E$ are infrared active modes and $B_2 + E$ correspond at acoustic modes. In contrast the $3A_2$ is a remained silent mode.

Table 3: Group Theory analysis of D_{2d} factor group to $AB'B''O_6$ compounds.

ions	Wickoff sites/Symmetry	Irreducible Representations
A	$2c/C_{2v}$	$A_1 \oplus B_2 \oplus 2E$
B'	$2c/C_{2v}$	$A_1 \oplus B_2 \oplus 2E$
B''	$2c/C_{2v}$	$A_1 \oplus B_2 \oplus 2E$
O	$4e/C_s$	$2A_1 \oplus A_2 \oplus B_1 \oplus 2B_2 \oplus 3E$
O	$4e/C_s$	$2A_1 \oplus A_2 \oplus B_1 \oplus 2B_2 \oplus 3E$
O	$4e/C_s$	$2A_1 \oplus A_2 \oplus B_1 \oplus 2B_2 \oplus 3E$
$\Gamma_T = 9A_1 \oplus 3A_2 \oplus 3B_1 \oplus 9B_2 \oplus 15E$		
$\Gamma_R = 9A_1 \oplus 3B_1 \oplus 8B_2 \oplus 14E$		$\Gamma_{IR} = 8B_2 \oplus 14E$
$\Gamma_s = 3A_2$		$\Gamma_{ac} = B_2 \oplus E$

The drawback in this methodology is its use in only polarized light. Since our samples are ceramics or powder, in consequence without crystal axis orientation, it is impossible to perform polarized measurements in order to discuss the vibrational modes in terms of irreducible factor groups. The more appropriated method is analysis in and out modes into structures. Both pyrochlore and trirutile structures are composed of octahedron networks BO_6 (and BO_6 or $B/B'O_6$) and cations A (and B or B/B').

In general the vibration modes of octahedron are observed between $300-900\text{ cm}^{-1}$ whereas extern mode frequencies are observed below 300 cm^{-1} . In this case we should make a correlation table symmetry for lattice, sub-lattice and lattice itself, like showed in **Table 2**. However, we should know what and how much internal modes are allowed in a free octahedron for subsequent analyses by Group Theory based on symmetry reduction of octahedron inside lattice by correlation of crystal structures in study. The Group Theory calculation of vibrational modes of molecules type XY_6 is showed in Apendixe B of Reference [22]. The distribution of the 21 degree of freedom of octahedral molecule is given by

$$\Gamma_v = A_{1g}(\nu_1) \oplus E_g(\nu_2) \oplus 3F_{1u}(T, \nu_3, \nu_4) \oplus F_{1g}(L) \oplus F_{2g}(\nu_5) \oplus F_{2u}(\nu_6)$$

where ν_1, ν_2 e ν_3 modes are stretching moves of B'' bonds, and ν_4, ν_5 and ν_6 angular deformations O - B'' - O. The libration octahedra modes $L(F_{1g})$ and ν_6 that originally are silent in both Raman and IR spectra can be observed due lowering local symmetry octahedra when put in a crystalline lattice. How is the $LiTaWO_6$ case considering its $P\bar{4}2_1m$ Space Group, like shown in the **Table 4**. The $B''O_6$ that originally was in the cubic symmetry O_h is in the C'_{2v} now. In consequence, it make $L(F_{1g})$ and ν_6 active in both Raman and IR spectra.

This methodology has a limitation that all $B''O_6$ octahedra to be un-connected themselves, although all $B'O_6$ are connected. The vibrational activity for boths octahedra depend of bond forces $B' - O$ and $B'' - O$. In this case, the B'' cation has more eletrovalence and make the $B'' - O$ constant force stronger than $B' - O$. In the case of both constants forces are approximately close themselves, we can observe both octahedral activities.

Catti et. al.[23] study the thermal, structural, vibrational and electrical properties of $HTaWO_6 \cdot xH_2O$ ($x = 3/2, 1/2, 0$). The results obtained through X-ray showed that $HTaWO_6 \cdot 3/2H_2O$ belongs to tetragonal system with lattice parameters $a = 4.710 \text{ \AA}$ and $a = 25.80 \text{ \AA}$.

The **Figure 3** show $LiTaWO_6$ Raman spectrum at room temperature. This spectrum is in agreement with one reported by Catti et.al.[11], showing a similarity between the samples. Inspite that, there is no deep discusion about observed vibration modes, due the absence of the $LiTaWO_6$ monocrystals. There is a only reference about 960 cm^{-1} band, which has been attributed to TaO_6 octahedra stretch vibration that share sides.

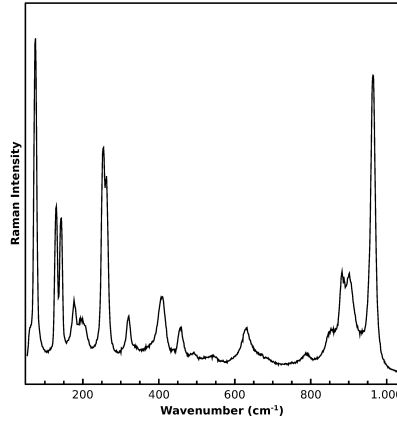


Figure 3: $LiTaWO_6$ Raman Spectrum at room temperature.

Not all predicted modes have been observed in the Raman spectrum, maybe sobreposition of some bands, or due low polarizability of some modes. Thus, the amount of bands and their line widths are consistent with ordered crystalline structure where atoms occupy positions of low symmetry.

Table 4: Correlation for $AB'B''O_6$ with D_{2d} point group. Raman (R), Infrared (IR), and Silent modes (S).

<i>ion/sym. free ion</i>	<i>site symmetry</i>	<i>cel. unit. symm</i>	<i>vibrational – modes – activity</i>
$A, B' / -$	$cC'_{2v}(2)$	D_{2d}	
	$(2Tz)A_1$	A_1	$\rightarrow 9A_1(3T, \nu_1, \nu_2, \nu_3, \nu_4, \nu_5, \nu_6) - R$
	$(2Tx)B_1$	A_2	$\rightarrow 3A_2(L, \nu_5, \nu_6) - S$
	$(2Ty)B_2$	B_1	$\rightarrow 3B_1(L, \nu_5, \nu_6) - R$
$B'' O_6/O_h$	$cC'_{2v}(2)$		
$(\nu_1)A_{1g}$	A_1	B_2	$\rightarrow 9B_2(2T, \nu_1, \nu_2, \nu_3, \nu_4, \nu_5, \nu_6, ac) - R, IR$
$(\nu_2)E_g$	A_1	E	$\rightarrow 15E(5T, 2L, \nu_2, 2\nu_3, 2\nu_4, \nu_5, \nu_6, ac) - R, IR$
$(R)F_{1g}$	A_2	B_1	
$(T, \nu_3, \nu_4)3F_{4g}$	A_2	B_2	
$(\nu_5)F_{2g}$	B_1	E	
$(\nu_6)F_{2u}$	B_2	E	

4.1 FTIR and Raman spectra comparison

In the Figure 4 are compared both IR transmittance (reproduced by Ref [12]) and Raman spectrum of $LiTaWO_6$ measured at room temperature. With respect to infrared spectrum, we can observe ten bands localized on 320, 390, 410, 451, 510, 660, 760, 885, 910, and 966 cm^{-1} . Note that, a lot of these bands have a clear correlation with some Raman spectrum bands, that is expected if we take into account a non-center-symmetric structure. In fact, according to Bhuvanesh et al. [10], this compound exhibits second harmonic generation, an exclusive property of polar materials, whose inversion of symmetry center is absent. For these results, the more probable structure for $LiTaWO_6$ is $P\bar{4}2_1m$.

Although we did not have oriented monocrystals of $LiTaWO_6$, we could do a qualitative analysis of the Raman modes observed based on both octahedra ($B''O_6$) and cations lattice vibrations in the structure. Since the W-O bond lengths are approximately equal to Ta-O bonds, the vibrational spectrum of $LiTaWO_6$ can be dominated mainly by WO_6 or TaO_6 octahedron vibrations. In some cases, if charges or masses of B' or B'' are very different, it should be possible to make a differentiation between vibrations of $B'O_6$ and $B''O_6$. In general, the frequency order of bonds stretching is $\nu_1 > \nu_3 \geq \nu_2$, while for frequencies of angular deformations O-B''-O is $\nu_4 \geq \nu_5 > \nu_6$. In the $LiTaWO_6$ structure the WO_6 or (TaO_6) structure are slightly distorted, leaving themselves to lower symmetry C_{2v} , than pyrochlore one (D_{3d}). The influence of octahedral symmetry lowering in the vibrational spectrum should be analyzed using a correlation diagram like is shown in the Table 2. In accordance with Table 2 we observed 21 Raman modes that correspond to octahedra internal modes ($2\nu_1, 3\nu_2, 4\nu_3, 4\nu_4, 4\nu_5, 4\nu_6$) of which thirteen ($\nu_1, 2\nu_2, 3\nu_3, 3\nu_4, 2\nu_5, 2\nu_6$) must be observed for both Raman and infrared, while the remaining only observed by Raman spectroscopy.

In accordance with literature, for compounds containing tantalum and tungsten, like perovskite, for example, $LiTaO_3$ [24], A_2InTaO_6 ($A = Ba, Sr$) [25], A_2CoWO_6 ($A = Ba, Sr$) [26] and $A_3In_2WO_9$ ($A = Ba, Sr$) [27], the wavenumbers of the symmetrical breath of the octahedra TaO_6 and WO_6 have values of 840 cm^{-1} . Based on it, the unusual characteristic of the $LiTaWO_6$ spectrum are bands localized between 810 and 1000 cm^{-1} . Similar characteristics are observed on $TiTa_2O_7$ [28] and $TiNb_2O_7$ [29], that have two octahedra distributions of MO_6 ($M = Ta$ e Nb), respectively; one with the shared vertex MO_6 and other with shared edges (M_2O_{10}). Two intense bands were observed in 899 and 1020 cm^{-1} for the $TiTa_2O_7$ and 1000 and 892 cm^{-1} for the $TiNb_2O_7$ compounds. The first was attributed to molecular breath symmetric mode M_2O_{10} , while the second was designed like a molecular breath symmetric of the M_2O_{11} unit. The wavenumber differences between the two bands were 121 and 180 cm^{-1} for $TiTa_2O_7$ and $TiNb_2O_7$, respectively. If this wavenumber difference is systematic for the octahedra shared vertex and edge, the corresponding Raman bands are 964 and 851 cm^{-1} (See Figs. 3 and 4), which difference is 113 cm^{-1} . It may be indicative that TaO_6 and WO_6 are well correlated. There is also a doublet to assign; it is centered in 890 cm^{-1} . Since the crystalline system of octahedra TaO_6 and WO_6 in the trirutile structure is different from the perovskites, we expected a displacement of the wavenumber of the vibrations of these octahedra, what it implies the 890 cm^{-1} doublet may be a symmetric stretching (ν_1) of the isolated octahedra TaO_6 and WO_6 .

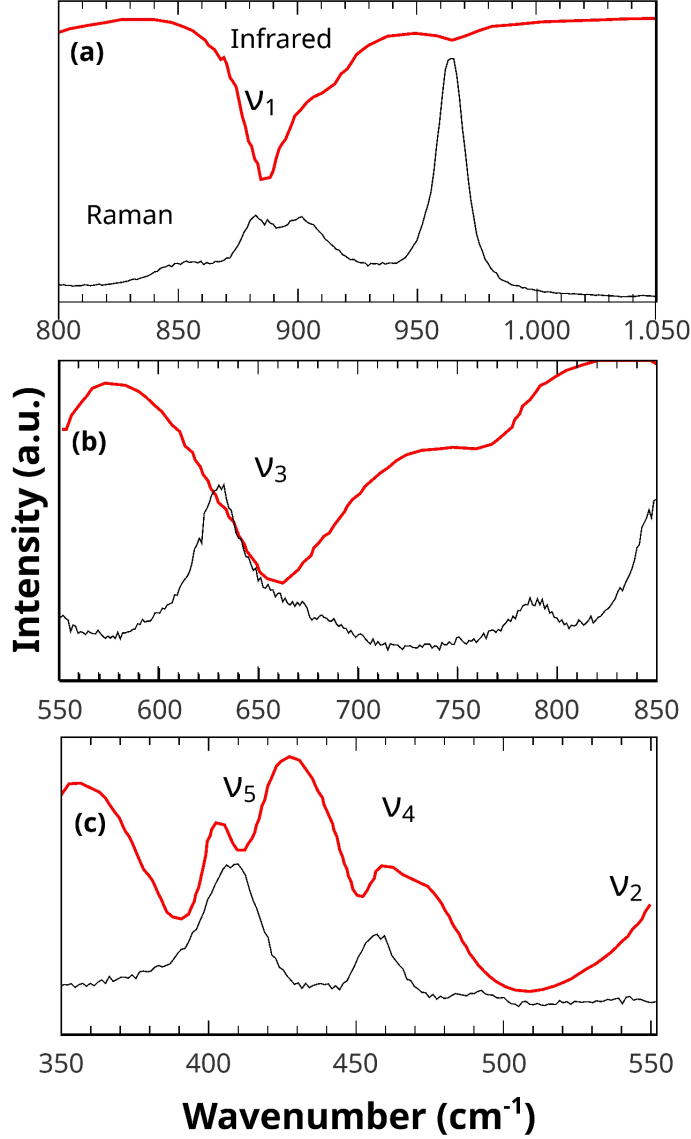


Figure 4: Comparison between Raman and infrared spectra of LiTaWO_6 between (a) $800\text{-}1050\text{ cm}^{-1}$, (b) $550\text{-}840\text{ cm}^{-1}$ and (c) $350\text{-}550\text{ cm}^{-1}$ ranges.

In the next spectral region, showed in the **Figure 4(b)**, we can observe two bands in 600 and 760 cm^{-1} in the infrared spectrum and three bands in the Raman spectrum in 630 , 670 and 785 cm^{-1} . In general, in this region is localized the assymmetric stretching of infrared active mode ν_3 . Lavat and Baran [30] studied infrared spectra of several perovskites containing tantalum as manly octahedral unit and observed that this mode is localized on 650 and 670 cm^{-1} region. On the other hand, Liegeois-Duyckaerts and Tarte[31] studied the Raman and infrared spectrum of the other series of perovskites containing tungstein as mainly octahedral unit and observed that $\nu_3(\text{WO}_6)$ occurred in the $600\text{-}650\text{ cm}^{-1}$ region. Based on this, we can only assign the bands between 650 cm^{-1} to $\nu_3(\text{WO}_6)+\nu_3(\text{TaO}_6)$. Despite of suppositions, we can not assign the $750\text{-}810\text{ cm}^{-1}$ bands based on the free octahedra, but we can suppose this vibrations have origin in movements of couple (TaWO_{11}) or by (TaWO_{10}) octahedra.

The **Figure 4(c)** show the Raman and Infrared spectra comparison in the $350\text{-}570\text{ cm}^{-1}$ region. In this spectral region are concentrated stretching anti-symmetric modes of M - O (ν_2) bonds, and angular deformations of O-M-O angles, with symmetry of ν_4 and ν_5 modes of the free octahedron. In according to literature, the $\nu_4(\text{TaO}_6)+\nu_4(\text{WO}_6)$, $\nu_5(\text{TaO}_6)+\nu_5(\text{WO}_6)$ e $\nu_2(\text{TaO}_6)$ modes have energy in the regions of $330\text{-}450\text{ cm}^{-1}$ [30, 31], $375\text{-}450\text{ cm}^{-1}$

[25, 31] and 550 cm^{-1} [25]. We observed five and six bands in infrared and Raman spectra, respectively. In general, the ν_2 mode have low intensity [25] and in lot of cases is not observed [31] in Raman spectrum, however we can assign the 537 cm^{-1} band in the LiTaWO_6 Raman spectrum as $\nu_2(\text{TaO}_6)$ symmetric mode. The wide band centering in 510 cm^{-1} is very comom in a lot of compounds of perovskites family [27, 30] having ν_4 symmetry mode, thus we assign the bands between $430\text{-}520\text{ cm}^{-1}$ as a ν_4 symmetry modes. Finally the bands localized between $375\text{-}425\text{ cm}^{-1}$ are vibrations of ν_5 symmetry.

The bands lower than 375 cm^{-1} are the most difficult to indentify because in this region are localized the librational (L) and translational (T) modes of crystal lattice. In this case, we consider the movement of the cations Li, Ta and W at long x , y or z directions, as showed in the Table 2. Through the results of the Group Theory shown in this papper we must observe sixteen modes ($10T+3L+3\nu_6$) in this spectral region. Due the degenerescence of some bands or the weak intensity of the Raman spectrum due a material polarizability, we only observe ten bands in this region.

5 Raman spectrum of the $\text{H}_{0.833}\text{Li}_{0.167}\text{TaWO}_6$ trirutile

Figure 5 shows the Raman Spectra of the $\text{H}_{0.833}\text{Li}_{0.167}\text{TaWO}_6$, LiTaWO_6 , and $\text{HTaWO}_6 \cdot n\text{H}_2\text{O}$ [12]. The Raman spectra of the $\text{H}_{0.833}\text{Li}_{0.167}\text{TaWO}_6$ and $\text{HTaWO}_6 \cdot n\text{H}_2\text{O}$ show some differences with LiTaWO_6 for both the number of bands and bandwidth.

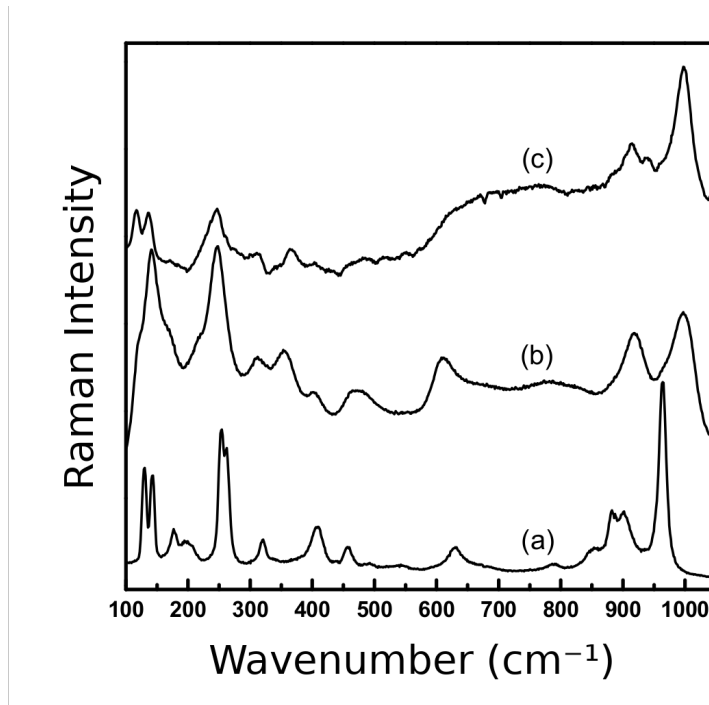


Figure 5: Raman spectra of the trirutile compounds: (a) LiTaWO_6 sample, (b) $\text{HTaWO}_6 \cdot n\text{H}_2\text{O}$ [35] and (c) doped sample $\text{H}_{0.833}\text{Li}_{0.167}\text{TaWO}_6$.

The Raman spectrum of **Figure 5(b)** is well represented for $\text{HTaWO}_6 \cdot n\text{H}_2\text{O}$ trirutile with n between $3/2$ and $1/2$ like shown in the reference [11]. We can see the band shift of higher energy to high wavenumbers.

When hydration of $\text{HTaWO}_6 \cdot n\text{H}_2\text{O}$ increases the structure tend to become more open with c lattice parameter changing from 20 to 26 \AA [18, 32]. While with the Li^+ ion the structure tends to more closely, with c lattice parameter remaining to 9.30 \AA . The supercell formation also is attributed the translation of the interlayers of the water molecules, perpendicular to the c axis, that are oriented to optimize the hydrogen bonds that connected to adjacent layers [19]. The detailed analysis of the characteristic of the ionic exchange reactions had been shown for some authors. They took into account the ionic exchange reactions Li^+/H^+ occur followed by unit cell change, from tetragonal primitive to body center tetragonal ($\text{HTaWO}_6 \cdot n\text{H}_2\text{O}$) [18]. According to Kumada et.al. [19] the $\text{Li}_{0.9}\text{H}_{0.1}\text{TaWO}_6$ compound, have lattice parameter $c=11.1\text{ \AA}$ that is close to the LiTaWO_6 due to the large Li^+ ion concentration. As $\text{H}_{0.833}\text{Li}_{0.167}\text{TaWO}_6$ has

low Li^+ concentration, it is expected that the vibrational spectrum of this compound resembles that of $\text{HTaWO}_6 \cdot n\text{H}_2\text{O}$, as observed in **Figure 5**.

Although the $\text{HTaWO}_6 \cdot n\text{H}_2\text{O}$ have the trirutile structure with c lattice parameter almost three times c lattice parameter of the LiTaWO_6 compound, we still see a strong disorder in the octahedral cations Ta^+ and W^+ due to the enlargement of the high wavenumber bands (more than 500 cm^{-1}), taking as reference the LiTaWO_6 Raman spectrum.

As the H^+ and Li^+ ions contribute only to lattice libration modes (less than 500 cm^{-1}) in the wavenumber interval showed in **Figure 5**, we observe a remarkable difference in this spectrum region.

6 Conclusion

We can summarize that studies that indicate a non-symmetric $\text{P}\bar{4}2_1m$ structure can be performed, although done in a polycrystalline sample. Even so, we conducted a qualitative study using the knowledge about Raman modes of TiTa_2O_7 and TiNb_2O_7 by comparison.

The prediction by Group Theory for both IR and Raman active modes are 13 ($\nu_1, 2\nu_2, 3\nu_3, 3\nu_4, 2\nu_5, 2\nu_6$) from the total of 21 internal Raman modes ($2\nu_1, 3\nu_2, 4\nu_3, 4\nu_4, 4\nu_5, 4\nu_6$). With respect to the infrared spectrum, we observed ten bands localized on 320, 390, 410, 451, 510, 660, 760, 885, 910, and 966 cm^{-1} , with a lot of these bands, have a clear correlation with some Raman spectrum bands, that is expected to a non-center-symmetric structure, as described by Bhuvanesh et.al.[10].

As long as there is no significant difference between $\text{B}'\text{O}_6$ and $\text{B}''\text{O}_6$ mass and charge, the band frequencies of $\text{B}'\text{O}_6$ and $\text{B}''\text{O}_6$ are closely each other, like a consequence of both $\text{B}'\text{-O}$ and $\text{B}''\text{-O}$ are approximately equal. It is a case of Ta-O and W-O bonds. As a consequence, the vibrational spectrum of LiTaWO_6 is dominated mainly by WO_6 and TaO_6 octahedron vibrations. Take into account the frequency order of bonds stretching is $\nu_1 > \nu_3 \geq \nu_2$, while for frequency order of angular deformations $\text{O-B}''\text{-O}$ is $\nu_4 \geq \nu_5 > \nu_6$, we can assign:

- ν_1 to 851 and 964 cm^{-1} ;
- The 510 cm^{-1} band belong to ν_4 , as well as the bands localized between $430\text{-}520 \text{ cm}^{-1}$;
- The ν_5 bands are localized between $375\text{-}425 \text{ cm}^{-1}$;
- The bands lower than 375 cm^{-1} are more difficult to identify. In this spectral region are localized the librational (L) and translational (T) modes.

We can observe ten infrared bands, (320, 390, 410, 451, 510, 660, 760, 885, 910, and 966 cm^{-1}), of which 8 we can assign for both Raman and infrared activity.

Although this procedure is very limited, we can assign some vibrational bands for both Raman and infrared activity, with a significant level of confidence to conclude that our sample belongs to $\text{P}\bar{4}2_1m$ Space Group.

7 Acknowledgments

D. Valim acknowledge E.N. Silva for his conversations about Group Theory and vibrational modes. D. Valim, AG Souza Filho, JM Filho, OL Alves, M.A.C. de Santis, and E.N. Silva acknowledge the Brazilian agencies, CNPq, CAPES, FUNCAP, and FAPESP for financial support.

References

- [1] A Bolzan, C Fong, B J Kennedy, and C J Howard. . *Acta Crystallographica, Section B*, B53:373–380, 1997.
- [2] J. I. Martínez, H. A. Hansen, J. Rossmeis, and J. K. Nørskov. Formation energies of rutile metal dioxides using density functional theory. *Physical Review B - Condensed Matter and Materials Physics*, 79(4):1–5, 2009.
- [3] Angel M. Arevalo-Lopez, Elizabeth Castillo-Martinez, and Miguel Ángel Alario-Franco. A Study of $[\text{Cr-O6}]$ -based rutile analogues by means of EELS. *MRS Proceedings*, 1148(January):1148–PP03–31, 2008.
- [4] B. R. Maddox, C. S. Yoo, Deepa Kasinathan, W. E. Pickett, and R. T. Scalettar. High-pressure structure of half-metallic CrO_2 . *Physical Review B - Condensed Matter and Materials Physics*, 73(14):1–9, 2006.
- [5] Nan Jiang and John C.H. Spence. Electron energy-loss spectroscopy of the O K edge of NbO_2 , MoO_2 , and WO_2 . *Physical Review B - Condensed Matter and Materials Physics*, 70(24):1–7, 2004.

- [6] D. T. Maimone, A. B. Christian, J. J. Neumeier, and E. Granado. Lattice dynamics of ASb_2O_6 ($A=Cu, Co$) with trirutile structure. *Physical Review B*, 97(10):1–11, 2018.
- [7] G Blasse and A D M de Pauw. Crystal structure of some $LiMe^{5+}Me^{6+}O_6$ compounds. *Journal of Inorganic and Nuclear Chemistry*, 32(12):3960–3961, 1970.
- [8] J L Fourquet, J A Le Bail, and P A Gillet. $LiNbWO_6$: Crystal structure of its two allotropic forms. *Materials Research Bulletin*, 23:1163–1170, 1988.
- [9] M Catti. Structural environment of Li^+ and H^+ in $LiTaWO_6$ and $HTaWO_6 \cdot H_2O$ trirutile ionic conductors. *ISIS Experimental Report*, (12834), 2002.
- [10] N S P Bhuvanesh, B R Prasad, C K Subramanian, and J Gopalakrishnan. Non-linear optical response of rutile-related oxides, $LiM(V)M(VI)O_6$, and their derivatives obtained by ion-exchange and intercalation. *CHEMICAL COMMUNICATIONS*, (3):289–290, FEB 7 1996.
- [11] M Catti, E Cazzanelli, C M Mari, and G Mariotto. Trirutile Phases of $HTaWO_6 \cdot xH_2O$. *J. Solid State Chem.*, 107:108–116, 1993.
- [12] M A Culhari de Santis. ESTRUTURA LAMELAR VERSUS ESTRUTURA PIROCLORO: OBTENÇÃO DE COMPOSTOS DO TIPO $H_{1-x}Ag_xTaWO_6$. Dissertação de mestrado, UNICAMP-Universidade Estadual de Campinas, 2006.
- [13] C M Mari, F Bonino, M Catti, R Pasinetti, and S. Pizzini. Electrical Conductivity of $HTaWO_6 \cdot H_2O$ and $HTaWO_6$. *Sol. Stat. Ion.*, 18-19:1013–1019, 1986.
- [14] S GARCIA-MARTIN, ML VEIGA, A JEREZ, and C PICO. Analisis de las propiedades de conductividade ionica em la estructura tipo pirocloro. *An. Quim. Int.*, 87:982–985, 1991.
- [15] S Zhuiykov. Hydrogen sensor based on a new type of proton conductive ceramic. *Int. J. Hydrogen Energy*, 21:749–759, 1996.
- [16] D Valim. *Espectroscopia vibracional e de impedância de $A_{1-x}A'_xTaWO_6 \cdot nH_2O$ ($A = H, Li, A' = Ag, H$)*. PhD thesis, Universidade Federal do Ceará, 2009.
- [17] Daniel Valim, Souza Filho AG, Filho JM, Alves OL, De Santis MAC3, and Silva EN. Vibrational and Thermal Properties of Ionic Conductors Type Pirochlore $H_{1-x}Ag_xTaWO_6 \cdot nH_2O$. *Journal of Material Sciences & Engineering*, 7(5), 2018.
- [18] V Bhat and J Gopalakrishnan. Novel layered oxides related to the rutile structure. Synthesis and investigation of ion-exchange and intercalation behaviour. *Solid State Ionics*, 26:25–32, 1988.
- [19] N Kumada, O Horiuchi, F Muto, and N Kinomura. A NEW LAYERED TYPE COMPOUND, $HTaWO_6 \cdot nH_2O$ ($n=0.5-1.5$) PREPARED FROM $LiTaWO_6$ BY ION EXCHANGE REACTION. *Mat. Res. Bull.*, 23:209–216, 1988.
- [20] N Kumada, M Takeshita, and N Kinomura. A NEW LAYERED TYPE COMPOUND, $HTaWO_6 \cdot nH_2O$ ($n = 0.5-1.5$) PREPARED FROM $LiTaWO_6$ BY ION EXCHANGE REACTION. *Mat. Res. Bull.*, 23:1053–1060, 1988.
- [21] L Sebastian and J Gopalakrishnan. Lithium ion mobility in metal oxides: a materials chemistry perspective. *J. Mater. Chem.*, 13:433–441, 2003.
- [22] E N Silva. *Propriedades vibracionais de perovskitas complexas ordenadas*. Tese de doutorado, Universidade Federal do Ceará, Fortaleza-CE, 2008.
- [23] M Catti and C M Mari. Raman Study and Electrical Conductivity of $HTaMO_6$ ($M=W$ and Te). *Sol. Stat. Ion.*, 40/41:900, 1990.
- [24] S M Kostritskii, P Bourson, M Aillerie, M D Fontana, and D Kip. Quantitative evaluation of the electro-optic effect and second-order optical nonlinearity of lithium tantalate crystals of different compositions using Raman and infrared spectroscopy. *Appl. Phys.*, B 82:423–430, 2006.
- [25] A Dias, L A Khalam, M T Sebastian, and R L Moreira. Raman-spectroscopic investigation of Ba_2InTaO_6 and Sr_2InTaO_6 perovskites. *Journal of Solid State Chemistry*, 180:2143–2148, 2007.
- [26] A P Ayala, I Guedes, E N Silva, M S Augsburg, M del C Viola, and J C Pedregosa. Raman investigation of A_2CoBO_6 ($A=Sr$ and Ca , $B=Te$ and W) double perovskites. *Journal of Applied Physics*, 101:123511, 2007.
- [27] E N Silva, A P Ayala, I Guedes, R M Pinacca S A Larregola, M del C Viola, and J C Pedregosa. Vibrational study of double perovskites $a_3in_2b''o_9$ ($a=ba, sr; b'' = u, w$). *Journal of Raman Spectroscopy*, 2009.
- [28] N G Eror and U Balachandran. Vibrational spectroscopic study of the compound $TiTa_2O_7$. *Spectrochim. Acta, Part A*, 39:261–263, 1983.

- [29] A A MCCONNELL and J S ANDERSON and C N R RAO. RAMAN-SPECTRA OF NIOBIUM OXIDES. *SPECTROCHIMICA ACTA PART A-MOLECULAR AND BIOMOLECULAR SPECTROSCOPY*, 32(5):1067–1076, 1976.
- [30] A E Lavat and E J Baran. IR-spectroscopic characterization of $A_2B'B_6O_6$ perovskites. *Vibrational Spectroscopy*, 32:167, 2003.
- [31] M LIEGEOIS and P TARTE. VIBRATIONAL STUDIES OF MOLYBDATES, TUNGSTATES AND RELATED COMPOUNDS .3. ORDERED CUBIC PEROVSKITES $A_2B_2B_2V_6O_{16}$. *SPECTROCHIMICA ACTA PART A-MOLECULAR AND BIOMOLECULAR SPECTROSCOPY*, A 30(9):1771–1786, 1974.
- [32] C M Mari, A Anghileri, M Catti, and G Chiodelli. . *Sol. Stat. Ion.*, 28-30:642, 1988.